Breast Cancer Research

17-allyamino-17-demethoxygeldanamycin treatment results in a magnetic resonance spectroscopy-detectable elevation in choline-containing metabolites associated with increased expression of choline transporter SLC44A1 and phospholipase A2

Breast Cancer Research 2010, **12**:R84 doi:10.1186/bcr2729

Alissa H Brandes (ahb2002@med.cornell.edu)
Christopher S Ward (christopher.ward@duke.edu)
Sabrina M Ronen (sabrina.ronen@ucsf.edu)

ISSN 1465-5411

Article type Research article

Submission date 23 July 2010

Acceptance date 14 October 2010

Publication date 14 October 2010

Article URL http://breast-cancer-research.com/content/12/5/R84

17-allyamino-17-demethoxygeldanamycin treatment results in a magnetic resonance spectroscopy-detectable elevation in choline-containing metabolites associated with increased expression of choline transporter SLC44A1 and phospholipase A2

Alissa H Brandes, Christopher S Ward, Sabrina M Ronen

Department of Radiology and Biomedical Imaging, University of California, San Francisco, 1700 4th St., San Francisco, CA 94158, USA

Corresponding author: Sabrina Ronen, email: Sabrina.Ronen@ucsf.edu

ABSTRACT

Introduction: 17-allyamino-17-demethoxygeldanamycin (17-AAG), a small molecule inhibitor of Hsp90, is currently in clinical trials in breast cancer. However, 17-AAG treatment often results in inhibition of tumor growth rather than shrinkage, making detection of response a challenge. Magnetic resonance spectroscopy (MRS) and spectroscopic imaging (MRSI) are noninvasive imaging methods than can be used to monitor metabolic biomarkers of drug-target modulation. This study set out to examine the MRS-detectable metabolic consequences of Hsp90 inhibition in a breast cancer model.

Methods: MCF-7 breast cancer cells were investigated, and MRS studies were performed both on live cells and on cell extracts. ^{31}P and ^{1}H MRS were used to determine total cellular metabolite concentrations and ^{13}C MRS was used to probe the metabolism of [1,2-^{13}C]-choline. To explain the MRS metabolic findings, microarray and RT-PCR were used to analyze gene expression, and *in vitro* activity assays were performed to determine changes in enzymatic activity following 17-AAG treatment.

Results: Treatment of MCF-7 cells with 17-AAG for 48 hours caused a significant increase in intracellular levels of choline (to 266 ± 18% of control, $P = 0.05$) and phosphocholine (PC; to 181 ± 10% of control, $P = 0.001$) associated with an increase in expression of choline transporter SLC44A1 and an elevation in the *de novo* synthesis of PC. We also detected an increase in intracellular levels of glycerophosphocholine (GPC; to 176 ± 38% of control, $P = 0.03$) associated with an increase in PLA2 expression and activity.

Conclusions: This study determined that in the MCF-7 breast cancer model inhibition of Hsp90 by 17-AAG results in a significant MRS-detectable increase in choline, PC and GPC, which is likely due to an increase in choline transport into the cell and phospholipase activation. ^{1}H MRSI can be used in the clinical setting to detect levels of total choline-containing metabolite (t-Cho, composed of intracellular choline, PC and GPC). As Hsp90 inhibitors enter routine clinical use, t-Cho could thus provide an easily detectable, noninvasive metabolic biomarker of Hsp90 inhibition in breast cancer patients.

INTRODUCTION

Recent reports from the American Cancer Society indicate that nearly 1 in 8 American women will be diagnosed with breast cancer in her lifetime. As the prevalence of this disease persists, increasing pressure is created to develop novel and improved therapies. Cancer research has become increasingly focused on the potential of various small molecule inhibitors targeting specific proteins in signaling pathways that are commonly overexpressed in cancer. While these drugs have had some success in clinical trials, they still have limited efficacy in treating many cancer types, largely due to cross-talk between different pathways, feedback loops and parallel signaling [1].

This challenge might be overcome by simultaneously inhibiting several oncogenic pathways; 17-allyamino-17-demethoxygeldanamycin (17-AAG), a small molecule inhibitor of Heat Shock Protein 90 (Hsp90), accomplishes this. Hsp90 is a molecular chaperone responsible for the folding and stability of multiple client proteins, many of which are oncogenes, including Akt, c-Raf, and Her-2 [2]. When 17-AAG inhibits Hsp90, its client proteins are degraded via the proteasome ubiquinitation pathway resulting in inhibition of oncogenic signaling. High expression of Hsp90 has also been associated with decreased survival in breast cancer [3]. Hsp90 inhibitors, including 17-AAG, are currently undergoing clinical trials and show promise as effective anti-cancer therapies for the treatment of many cancer types, including breast cancer [4, 5]. However, the treatment of tumors with 17-AAG most often results in an inhibition of tumor growth, rather than shrinkage [6-8]. As a result, early response to this type of treatment is near impossible to detect by traditional imaging, such as computed tomography (CT) and magnetic resonance imaging (MRI). As this therapy enters routine clinical use, it would

be beneficial to have a noninvasive functional or metabolic biomarker that could inform on the molecular effects of Hsp90 inhibition in patients.

Magnetic resonance spectroscopy (MRS)-detectable phosphocholine (PC) could potentially serve as such a biomarker. PC and in some cases GPC concentrations are elevated in tumors as compared to normal tissue, and have been shown to increase with increasing malignancy in breast cancer models and patient studies [9-15]. Accordingly, PC and total choline-containing metabolites (t-Cho, composed of choline, PC and glycerophosphocholine (GPC) and detectable by ^{1}H magnetic resonance spectroscopic imaging (MRSI)) are now recognized as clinically relevant metabolic biomarkers of breast cancer [14, 16, 17]. Additionally, ^{31}P and ^{1}H MRS studies have demonstrated that PC and t-Cho levels decrease in response to chemotherapy as well as targeted therapies, both *in vitro* and *in vivo* [18-28].

However, a previous MRS-based study examining the effects of 17-AAG in a colon cancer model reported the somewhat atypical effect of an increase in PC and GPC concentration following response to treatment [29]. This finding was supported by a different PET-based study, which reported an increase in uptake of the PET tracer [^{11}C]-choline after treatment with HSP90 inhibitor NVP-AUY922 in three different cell lines (MCF-7 human breast cancer, U87MG human glioblastoma and HCT116 human colon cancer) [30]. GPC levels have been shown to increase in response to other anticancer drug treatments [31-33].

The concentration of PC in the cell is regulated by the enzymes of the choline phospholipid metabolic pathway (Figure 1). Extracellular choline is actively transported into the cell by several choline transporters and is subsequently phosphorylated to PC by choline kinase (ChoK) [34, 35]. CTP:phosphocholine cytidylyltransferase (CCT) metabolizes PC to cytidine diphosphate-choline (CDP-choline). Diacylglycerol

cholinephosphotransferase (CPT) then further metabolizes CDP-choline to one of the main membrane phospholipids, phosphatidylcholine (PtdCho), with CCT being considered the rate-limiting step for PtdCho synthesis [36]. Various phospholipase enzymes can breakdown PtdCho: phospholipase A1 and A2 (PLA1 and PLA2) generate fatty acids and lyso-phosphatidylcholine (Lyso-PtdCho), which is further metabolized by lysophospholipase (LPL) into fatty acids and GPC; phospholipase C (PLC) generates PC and diacylglycerol; phospholipase D (PLD) generates choline and phospahtidic acid. GPC can also be further metabolized by glycerophosphocholine phosphodiesterase (GDPD) into choline. Examination of this pathway reveals three possible sources that could be responsible for increased PC following 17-AAG treatment: an increase in the *de novo* synthesis of PC from extracellular choline, a decrease in the further metabolism of PC via CCT, or an increase in breakdown of PtdCho.

Since 17-AAG is currently in clinical trials in breast cancer patients [4, 5], we set out to determine whether PC and t-Cho can serve as noninvasive biomarkers of Hsp90 inhibition in this group of patients. Our goal was first to confirm that treatment with 17-AAG results in an increase in PC and t-Cho, and second to investigate the underlying mechanism of their modulation. We studied the effect of 17-AAG treatment on the MCF-7 breast cancer cell line by probing choline metabolism using MRS and using complementary assays to determine the activity and expression of the enzymes involved in choline phospholipid metabollism. We found that 17-AAG caused an increase in the intracellular choline and PC concentrations, likely resulting from increased expression of the choline transporter SLC44A1 and elevation in the *de novo* synthesis of PC. We also found that GPC levels were elevated with 17-AAG treatment, resulting from an increase in gene expression and activity of PLA2.

MATERIALS AND METHODS

Cell Culture

MCF-7 cells were obtained from American Type Culture Collection via UCSF Cell Culture Facility (San Francisco, CA, USA). Cells were cultured in DMEM supplemented with 10% heat-inactivated fetal bovine serum, 2 mM L-glutamine, 100 units/ml penicillin and 100 μg/ml streptomycin (UCSF Cell Culure Facility). Custom-made DMEM with 0.22g/L inorganic phosphate (UCSF Cell Culture Facility) was used for all MRS experiments. For inhibition of Hsp90, 3 μM 17-AAG (LC Laboratories, Woburn, MA, USA) was added to the culture medium for a period of 48 hours. Medium was replenished with fresh 17-AAG every 24 hours during treatment.

The doubling time of MCF-7 cells in the logarithmic phase growing in tissue culture flasks or on beads was determined by seeding at a density of 1 x 10^6 cells/75 cm^2 flask or at a density of 3 x 10^6 cells/0.5 mL beads, trypsinizing at 24h intervals and counting the number of cells using a hemocytometer.

Cell Proliferation Assay

The effect of 17-AAG treatment on cell proliferation was determined using the WST-1 cell proliferation assay (Roche, Indianapolis, IN, USA). Cells were seeded in 96-well microplates (1.5 x 10^6 cells/well in 150 μL culture medium) and control and 17-AAG-treated cells probed at different time periods between 4 and 48 hours. For this cells were incubated for 1 hour with WST-1 reagent and cell viability was determined by quantification of the absorbance at 440 nm using a plate reader spectrophotometer (Tecan, Salzburg, Austria).

Protein Determination

Protein concentrations per cell were determined in cells lysed in Cell Lysis Buffer (Cell Signaling, Beverly, MA, USA) using a Coomassie Plus—The Better Bradford™ Assay Kit (Pierce, Rockford, IL, USA), with bovine serum albumim (BSA) used as a protein standard. Absorbance was measured at 595 nm using a platereader spectrophotometer (Tecan).

Western Blotting

The effect of 17-AAG on levels of client proteins was analyzed by Western blotting. Cellular lysates were extracted in Cell Lysis Buffer (Cell Signaling) with added Protease Inhibitor (Calbiochem, San Diego, CA, USA). Protein concentration was determined using Coomassie Plus Protein Assay (Pierce). Approximately 30 μg of protein was loaded into 4-20% SDS-PAGE gels (Bio-Rad, Hercules, CA, USA). Gels were run for 30 min and then proteins were electrotransferred onto nitrocellulose membranes. Membranes were blocked for one hour in 5% milk in TBST, and then incubated overnight with primary antibodies against Akt, c-Raf and Actin (Cell Signaling), with Actin used as a loading control. After incubation for two hours with secondary antibody anti-IgG horseradish peroxidase-linked antibody (Cell Signaling), the immunocomplexes were visualized using ECL Western Blotting Substrate (Pierce).

Flow cytometry

1 x 10^6 cells were seeded in 75 cm^2 tissue culture flasks in 10 mL of culture medium. Following treatment, approximately 2 x 10^6 cells were harvested by trypsinization, washed with PBS, and fixed in 70% ethanol. Fixed cells were incubated with RNase A at 100 units/ml (Sigma, St. Louis, MO, USA) for 30 min, washed with

PBS, and then stained with propidium iodide at 20 μg/ml (Sigma) for 30 min. Cells were counted using a FACS Calibur flow cytometer using CellQuest Pro software (BD Biosciences, Mountain View, CA, USA) and single cells were gated away from clumped cells using forward light scattering, on an FL2-width versus FL2-area dot plot. The percentage of cells in the G_1, S, and G_2/M phases was determined by plotting a histogram of FL2-A. The relative cell size of the G_1, S, and G_2/M phase populations of control and 17-AAG treated cells was determined using forward scattering height [FSC-H].

Perfused cell MRS Studies

Approximately 4 x 10^7 MCF-7 cells were grown on Biosilon microcarrier beads (NUNC, Rochester, NY, USA) in order to be loaded into a perfusion system for MRS studies as described previously [37]. Cells were seeded on the microcarrier beads, allowed to attach for 24 hours and then treated for 48 hours prior to the MR experiment. In order to monitor a similar number of cells during MRS acquisition, control cells were seeded at a density of ~5 x 10^6 cells/mL of beads and 17-AAG treated cells were seeded at a density of ~9 x 10^6 cells/mL of beads. An additional set of cells was seeded on beads for each experiment and treated in an identical fashion to those loaded into the perfusion system in order to obtain cell counts for both the start and end of the experiment.

MRS studies were performed on a 500-MHz INOVA spectrometer (Varian, Palo Alto, CA, USA). Composite pulse proton-decoupled ^{31}P spectra were first acquired to confirm cell viability and quantify metabolite levels. ^{31}P spectra were acquired using a 30° pulse and 3 second relaxation delay and 1000 transients for a total acquisition time of 70 minutes. Cells were then perfused with fresh culture medium containing only 56μM [1,2-^{13}C]-choline (Cambridge Isotope Laboratories, Andover, MA, USA) and no unlabeled choline for a period of 14 hours. Proton-decoupled (Waltz 16) ^{13}C spectra were

acquired during that time in 2-hour intervals using a 60° pulse and 6 second relaxation delay and 1024 transients. Spectra were quantified using ACD/Spec Manager version 9.15 software (Advanced Chemistry Development, Toronto, Ontario, Canada). Peak integrals obtained by deconvolution were normalized to cell number and to a metabolite of known concentration in the culture medium (1.87 μM inorganic phosphate (P_i) for ^{31}P spectra; 5 mM [1-^{13}C]-glucose (Cambridge Isotope Laboratories) for ^{13}C spectra). Data was corrected for saturation effects using correction factors obtained from a fully relaxed spectrum of perfused cells (fully relaxed ^{13}C spectra were acquired using a 90°, 20 μsecond pulse and 30 second relaxation delay for 1024 transients. Fully relaxed ^{31}P spectra were acquired using a 90°, 22 μsecond pulse and 30 second relaxation delay for 1000 transients).

Cell Extracts

Cells were grown in culture with medium in which all glucose and choline was completely replaced by 5 mM [1-^{13}C]-glucose and 56 μM [1,2-^{13}C]-choline (Cambridge Isotope Laboratories) for a period of 48 hours prior to extraction. Approximately 7 x 10^7 cells were extracted using the dual-phase extraction method, as described previously [26,[38, 39]. Briefly, cultured cells were collected by trypsinization, counted to obtain cell number, and fixed in 10 mL methanol. 10 mL of chloroform was added, followed by 10 mL of water. The solution was vortexed, centrifuged to separate the lipid and aqueous phases and then each phase was collected separately. Solvents were lyophilized off each sample. Aqueous samples were re-dissolved in a volume of 400 μL deuterium oxide and lipid samples were re-dissolved in 500 μL deuterated chloroform-methanol mixture.

^{13}C, ^{1}H and ^{31}P spectra were acquired on the lipid and aqueous portions of the cell extracts using a 600-MHz INOVA spectrometer (Varian) equipped with a 5-mm

broadband observe probe. Proton-decoupled (Waltz 16) ^{13}C and ^{31}P spectra were acquired using a 30° pulse and 3 second relaxation delay. ^{13}C aqueous spectra were acquired for 5000 transients and a total acquisition time of 6 hours. ^{13}C lipid spectra were acquired for 2500 transients and a total acquisition time of 3 hours. ^{31}P aqueous and lipid spectra were acquired for 2500 transients and a total acquisition time of 3 hours. ^{1}H spectra were acquired using a 90° pulse and 3 second relaxation delay and 256 transients for a total acquisition time of 25 minutes. Spectra were quantified using ACD/Spec Manager version 9.15 software (Advanced Chemistry Development). Peak integrals obtained by deconvolution were normalized to an external standard (100 mM trimethylsilyl propionate (TSP, Sigma) for ^{13}C spectra and 10 mM methylene diphosphoric acid (MDPA, Sigma) for ^{31}P spectra) and to cell number and corrected for saturation effects using data obtained from fully relaxed spectra of cell extracts as described above.

In addition, studies were performed with choline concentration at the normal concentration in human plasma. For this, cells were grown with a 10 μM choline concentration in the medium, and cells extracts and MRS experiments were performed as above.

Microarray analysis of gene expression

Total cellular RNA was isolated from approximately $1x10^7$ cells after 48 hours of treatment with 17-AAG or vehicle (DMSO) using the RNeasy Mini Kit (Qiagen, Valencia, CA, USA), according to manufacturer's instructions. RNA quality was determined by Bioanalyzer (Agilent, Santa Clara, CA, USA), considering RNA Intergrity Numbers (RIN) values of ≥8.0 acceptable (most values were 9.5 or higher). Microarray hybridization was performed at the UCSF Genomics Core Laboratories (UCSF/Gladstone, San Francisco, CA) using the Human Gene 1.0 ST. Human Gene

1.0ST was analyzed by fluorescence detection using the Agilent GeneArray Scanner (Agilent). Data acquisition was performed using the Micro Array Suite 5.0 software (Affymetrix, Santa Clara, CA, USA). Microarray experiments were performed with 4 repeats of each condition. Microarray data is available through the ArrayExpress public repository [EMBL:E-MTAB-339] in compliance with standards of the Microarray Data Gene Expression Society.

RT-PCR analysis of gene expression

RNeasy Mini Kit (Qiagen) was used to extract total cellular RNA from samples. Total RNA concentration of samples was determined using a ND1000 Fluorospectrometer (NanoDrop Technologies, Wilmington, DE, USA). The QuantiTect Reverse Transcription kit (Qiagen) was used to perform reverse transcription. Real-Time PCR was performed on the resulting cDNA on a Taqman 7900 (Applied Biosystems, Carlsbad, CA). Expression of ChoKα, ChoKβ and SLC44A1 were examined using Assays-on-Demand (Applied Biosystems) and normalized to the expression of the 18S ribosomal subunit (Integrated DNA Technologies, Coralville, IA, USA).

Choline Kinase Activity Assay

Choline kinase activity was measured in cell extracts by ^{1}H MRS as previously described [40]. In brief, approximately $1x10^{7}$ cells were re-suspended in 500 μL lysis buffer containing 100 mM Tris (pH 8.0), 1 mM EDTA and 10 mM DTT (all chemicals from Sigma). Lysate was repeatedly passaged through a fine-tipped needle (27 1/2G) for homogenization and was sonicated 10 x 1s at 20 kHz for membrane solubilization. The homogenate was centrifuged at 16,000 rpm for 30 minutes at 4°C, and 100 μL of reaction buffer containing 100 mM Tris (pH 8.0), 60 mM choline chloride, 120 mM ATP and 120

mM magnesium chloride (all chemicals from Sigma) at the final concentration was added to the lysate supernatant. MRS experiments were performed at 25°C on a 600-MHz INOVA spectrometer (Varian). The conversion of choline to PC was measured in an array of ^{1}H spectra over a one-hour period. ^{1}H spectra were obtained using a 90° pulse and 3 second relaxation delay. Choline and PC concentrations were determined as peak areas, and choline kinase activity was determined by linear regression analysis of points in the linear portion of the curve representing the time course of PC formation.

CTP:PC Cytidylyltransferase Activity Assay

This assay was based on the method outlined by Vance *et al*., 1981, with substantial modifications for compatibility with MRS [41]. In brief, 2 x 10^7 cells were resuspended in 540 μL lysis buffer containing 50 mM HEPES (pH 7.0) (Sigma), 5 mM EDTA (Sigma), 5 mM EGTA (Sigma), 5.5 mM sodium bisulfite (Sigma), and 1 μL/mL protease inhibitor cocktail (Calbiochem). Lysate was repeatedly passaged through a fine-tipped needle (27 1/2G) for homogenization and was sonicated 10 x 1s at 20 kHz for membrane solubilization. The homogenate was centrifuged at 16,000 rpm for 30 minutes at 4°C. The cytidylyltransferase activity of the supernatant fraction was measured immediately after addition of 60 μL reaction mixture (final concentrations: 50 mM Tris-HCl (pH 8.0), 10 mM cytidine triphosphate (CTP), 5 mM PC, 5 mM DTT and 25 mM $MgCl_2$) (all chemicals from Sigma). MRS experiments were performed at 33°C on the 600-MHz INOVA spectrometer (Varian). Proton-decoupled (Waltz 16) ^{31}P MR spectra were obtained using 30° pulse and 2.6 s repetition time. PC and CDP-choline concentrations were determined from peak areas. Cytidylyltransferase activity was determined by linear regression analysis of points in the linear portion of the curve representing the time course of CDP-choline formation.

Phospholipase C Activiy Assay

PtdCho-specific PLC activity was determined in cell lysates using the EnzChek Direct Phospholipase C Assay (Invitrogen, Carlsbad, CA, USA). The assay measures PLC activity by addition of a proprietary substrate (glycero-phosphoethanolamine with a dye-labeled sn-2 acyl chain), which is cleaved by PtdCho-specific PLC. The cleavage releases the dye-labeled diacylglycerol, which produces a positive fluorescence signal that can be measured. Fluorescence (485 nm excitation, 535 nm emission) was measured by SpectroFluor Plus spectrofluorometer (Tecan).

Phospholipase A1/A2 Activity Assay

The activity of PtdCho-specific PLA1 and PLA2 enzymes were determined in cell lysates using the EnzCheck Phospholipase A_1 and Phospholipase A_2 Assay kits (Invitrogen). The assay measures PLA1 activity by addition of a proprietary substrate (dye-labeled glycerophosphoethanolamines with BODIPY® FL dye-labeled acyl chain at the *sn*-1 position and dinitrophenyl quencher-modified head group). The *sn*-1 ester linkage of the substrate is cleaved by PLA1, which releases the dye-labeled acyl chain and produces a positive fluorescence signal that can be measured. The PLA2 activity assay measures the *sn*-2 ester link hydrolysis of the proprietary substrate 1-O-(6-BODIPY®558/568-aminohexyl)-2-BODIPY®FL C5-Sn-glycero-3-phosphocholine by PLA2 enzyme, which releases the dye-labeled portion and produces a positive fluorescent signal that can be measured. Fluorescence (505 nm excitation, 515 nm emission) was measured by SpectroFluor Plus spectrofluorometer (Tecan).

Statistical Analysis

Two-tailed Student's *t* test was used to determine the statistical significance of the results, with $P \leq 0.05$ considered significant. All results are expressed as mean ± standard deviation.

RESULTS

17-AAG treatment depletes Hsp90 client proteins and inhibits cell proliferation

Because our studies involved investigations of cells grown in flasks or on beads , we first confirmed that the proliferation rate of the cells was unaffected by the culture conditions. MCF-7 cells culture in 75-cm^2 flasks had a doubling time of 29.5 ± 3.7 hours (n=4), and this was comparable to a doubling time of 32.8 ± 2.7 hours for MCF-7 cells seeded on microcarrier beads (n=4, p=0.20). Of note, the doubling time of MCF-7 cells provided by American Type Culture Collection (from where the cells were obtained) is 29 hours and is consistent with our findings.

MCF-7 cells were treated for 48 hours with 3 μM 17-AAG. This led to depletion of the known Hsp90 client proteins total-Akt and c-Raf (Figure 2a) and was associated with a drop to 52±3% in the number of cells as compared to control (Figure 2b).

To further investigate the effect of 17-AAG treatment, FACS cell cycle analysis was performed after treatment for 48 hours. The results showed that the inhibitory effect of 17-AAG on cell proliferation is largely due to cell cycle arrest in the G_2/M phase. The fraction of cells in the G_2 phase increased from 8.4±4.2% in control cells to 44.7±5.2% in 17-AAG treated cells (n=3, p=0.0008). The fraction of cells in the S phase decreased from 31.2±2.3% in control cells to 4.6±3.1% in 17-AAG treated cells (n=3, p=0.0005). The fraction of cells in G_1 phase was not significantly altered by 17-AAG treatment and was 61±5% in control cells and 51±7% in 17-AAG treated cells (n=3, p=0.12).

Changes in relative cell size with 17-AAG treatment were also assessed. While there was an increase in the size of cells in the G_1 and S phase with 17-AAG treatment, there was a decrease in the size of cells in the G_2/M phase population. Thus, when considering the entire cell population, the average cell size was not significantly altered, with 17-AAG treated cells 104±4% the size of control cells (n=3, p=0.26). Consistent with this finding, average protein per cell was not significantly altered with 17-AAG treatment and was 2.76±0.05 mg/10^7 cells in control cells and 2.88±0.25 mg/10^7 cells in 17-AAG treated cells (n=3, p=0.12).

17-AAG treatment leads to increased PC levels and increased de novo PC synthesis

In order to assess the effects of 17-AAG treatment on choline metabolism in live cells, ^{31}P and ^{13}C MR spectra were acquired from MCF-7 cells grown on beads and perfused in a 10 mm NMR tube inside the spectrometer. First, a ^{31}P MR spectrum was acquired in order to determine the total PC pool in both control and 17-AAG-treated cells (Figure 3a). PC concentrations increased significantly to 180±19% of control in MCF-7 cells treated for 48 hours (n=3, p=0.004). Control cells had 19.3±3.4 femtomoles (fmol)/cell and 17-AAG-treated cells had 34.7±2.8 fmol/cell. Additionally, the concentration of GPC increased significantly with 17-AAG treatment to 216±56% of control, from 2.5±1.0 fmol/cell in control cells to 5.5±1.3 fmol/cell in 17-AAG treated cells (n=3, p=0.04). There was no significant change in the β-NTP levels after 17-AAG treatment, which were 104±12% of control (n=3, p=0.77).

The metabolism of live MCF-7 cells was then probed in real time by replacing choline in the medium with **only** [1,2-^{13}C]-choline and using ^{13}C MRS to monitor the buildup of PC over a 14-hour period (Figure 3b). The data curve obtained displays the build-up of ^{13}C-labeled PC inside the cells (Figure 3c). The level of ^{13}C-labeled PC after

14 hours of exposure to labeled substrate was significantly higher in the cells treated with 17-AAG. It increased with treatment to 171±39% of control, from 14.2±2.5 fmol/cell to 24.3±1.6 fmol/cell (n=3, p=0.007). Relative to the total PC concentrations determined from the ^{31}P spectrum, after 14 hours of labeling 75±17% of the PC pool was ^{13}C-labeled in control cells and 71±10% of the pool was labeled in 17-AAG treated cells, with no significant difference in percent labeling between control and treated (n=3, p=0.75).

At the end of the experiment, cells were extracted directly from the beads in order to assess ^{13}C-label incorporation into PtdCho (the lipid cannot be detected in live cells due its low mobility within the cell membrane) [38, 39]. After 14 hours, less than 10% of the PtdCho pool was ^{13}C-labeled and no [1,2-^{13}C]-GPC peak was observed in either the control or treated samples. We thus concluded that the build-up of [1,2-^{13}C]-PC observed over the first 14 hours was mainly due to the *de novo* synthesis of PC from extracellular labeled choline rather than PtdCho breakdown.

The initial rate of PC synthesis was linear over the first 8 hours and was quantified for both control and 17-AAG treated cells using linear regression (R=0.935 for control and R=0.982 for treated). This analysis showed that the initial rate of PC synthesis increased significantly to 184±7% of control with 17-AAG treatment, from 1.2±0.1 fmol/cell/hr in control cells to 2.3±0.4 fmol/cell/hr in treated cells (n=3, p=0.003). This increase was comparable to the increase observed in the total PC pool (180±19% of control) indicating that increased *de novo* synthesis of PC is the major cause of PC elevation following 17-AAG treatment.

17-AAG does not affect PtdCho levels but increases total and de novo GPC and intracellular choline levels

^{1}H ,^{31}P and ^{13}C MRS were used to quantify cellular metabolites in cell extracts following exposure to [1,2-^{13}C]-choline for 48 hours in order to further confirm the observations made in live cells, and to monitor *de novo* synthesis of PtdCho and GPC.

Data from the extracts confirmed the findings from live cells: after 48 hours of treatment with 17-AAG, the total PC levels increased to 181±10% relative to control, from 19.6±1.2 to 35.4±0.2 fmol/cell (n=3, p=0.001) (Figure 4a) and the *de novo* [1,2-^{13}C]-PC levels increased significantly to 165±10% of control, from 18.5±1.6 fmol/cell to 30.6±2.7 fmol/cell (n=3, p=0.006) (Figure 4b). Thus, after 48 hours of ^{13}C labeling, the PC pool was essentially fully ^{13}C labeled, with 94±3% of the pool labeled in control cells and 86±11% of the pool labeled in the treated cells and no significant difference in the percent of pool labeled between control and treated (n=3, p=0.20).

The concentration of total PtdCho was not changed significantly by 17-AAG treatment, with 25.2±4.1 fmol/cell in control cells and 26.3±4.0 fmol/cell in 17-AAG treated cells (n=3, p=0.75) (Figure 4c). *De novo* synthesized [1,2-^{13}C]-PtdCho levels were not significantly altered either. [1,2-^{13}C]-PtdCho levels in 17-AAG treated cells were 88±11% of control, with 11.8±2.6 fmol/cell in control cells and 10.3±0.9 fmol/cell in 17-AAG treated cells (n=3, p=0.44). After 48 hours, there was 46±3% incorporation of ^{13}C label into the total PtdCho pool in control cells and 40±4% incorporation into the total pool in 17-AAG treated cells, with no significant difference in the percent of total PtdCho pool labeled between control and treated (n=3, p=0.06).

As in live cells, GPC levels increased significantly to 176±38% relative to control (n=3, p=0.03). Control cells had 4.4±0.9 fmol/cell and 17-AAG-treated cells had 7.7±1.3 fmol/cell (Figure 4a). *De novo* GPC levels also significantly increased with 17-AAG treatment to 149±15% of control, from 1.9±0.1 to 2.8±0.3 fmol/cell (n=3, p=0.01) (Figure 4b). Of note, the difference between GPC levels determined in intact cells and in

extracts was not significantly different ($p>0.05$). After 48 hours, there was 44±11% incorporation of ^{13}C label into the total GPC pool in control cells and 37±5% incorporation into the total pool in 17-AAG treated cells, with no significant difference in the percent of total GPC pool labeled between control and treated (n=3, p=0.36).

The concentration of total intracellular choline was determined by quantification of the ^{1}H spectra (Figure 4d). Intracellular choline levels were significantly increased following 17-AAG treatment to 266±18% of control, from 0.5±0.1 fmol/cell in control cells to 1.3±0.4 fmol/cell in treated cells (n=3, p=0.05). Consistent with these findings, intracellular [1,2-^{13}C]-choline (as detected by ^{13}C MRS (Figure 4b)) was also increased in treated cells to 220±27% of control, from 0.6±0.1 fmol/cell in control cells to 1.2±0.3 fmol/cell in treated cells (n=3, p=0.05). Thus, after incubation with medium containing [1,2-^{13}C]-choline for 48 hours, the intracellular choline pool was essentially fully ^{13}C labeled. There was 116±53% ^{13}C enrichment of the intracellular choline pool in control cells and 95±38% ^{13}C enrichment in treated cells, with no significant difference in percent enrichment between control and treated (n=3, p=0.6).

17-AAG causes modulation in gene expression and activity of enzymes in the choline phosolipid metabolic pathway

In an effort to interpret the metabolic findings, microarray analysis was performed to determine the changes in gene expression associated with Hsp90 inhibition that could explain the alterations in choline metabolism observed following 17-AAG treatment. Table 1 lists the microarray data for enzymes involved in choline phospholipid metabolism.

Choline Transporters

Microarray analysis did not show significant changes in the gene expression of choline transporters SLC5A7, SLC22A1 or SLC22A2. However it did show a significant increase in the mRNA expression of the choline transporter SLC44A1. RT-PCR confirmed the microarray data, with a significant increase in SLC44A1 mRNA levels to 169±33% of control (n=4, p=0.04).

Choline kinase

Microarray analysis did not show any significant change in the expression of choline kinase α or β mRNA levels. RT-PCR was also performed to confirm the microarray data, and did not show a significant change in ChoKα or ChoKβ mRNA levels (n=4, p=0.2). Finally, the cellular activity of choline kinase remained essentially unchanged at 104±23% of control; control cell extracts incubated with choline produced 98±15 fmol PC/cell/hour and 17-AAG treated cells produced 102±37 fmol PC/cell/hour (n=4, p=0.51).

CTP:PC Cytidylyltransferase

Microarray analysis did not show any significant changes in gene expression of the CCT isoenzymes. The activity of CCT also remained unchanged with 17-AAG treatment at 107±21% of control; control cell extracts incubated with PC produced 18.2±5.3 fmol CDP-choline/cell/hour and 17-AAG treated cells produced 19.4±4.3 fmol CDP-choline/cell/hour (n=4, p=0.74).

Phospholipases

Genes coding for PtdCho-specific PLC isoenzymes have not yet been identified, preventing gene expression analysis; however, PtdCho-specific PLC activity was

assessed. The PtdCho-specific PLC activity assay performed on cell lysates showed a significant decrease in PLC activity with 17-AAG treatment to 66±10% of control (n=3, p=0.02).

Although there are many PLA isoenzymes, expression of PLA2G6, PLA2G10, PLA2G15, and PLA2G16 (all of which have activity on PtdCho) increased. Furthermore, the PtdCho-specific PLA1 and PLA2 enzyme activity assays did not find a significant increase in PLA1 activity, but did show a significant increase in PLA2 activity to 122±5% of control (n=3, p=0.02).

Finally, microarray data reported an increase in PtdCho-specific PLD1 expression to 137% of control. There was also an increase in mRNA levels of the GDPD isoenzymes GDPD2 and GDPD3 in the microarray; however, neither of these forms are known to be specific for GPC. No significant changes were found in the microarray for any of the LPL isoenzymes.

17-AAG leads to an increase in PC levels at physiological choline concentration

Choline is transported into the cell by several choline transporters, each with different affinities for choline and differing activities over a range of choline concentrations [34, 35]. Therefore, the overall rate of transport of choline into the cell may depend on the extracellular choline concentration. Since changes in expression of only one transporter were observed, we questioned whether 17-AAG would have the same effect on PC levels when extracellular choline concentrations are near physiological levels (more closely mimicking *in vivo* conditions). To address this question, MCF-7 cells were cultured in medium containing 10 μM choline (the concentration in human plasma) during the 48-hour treatment period [42, 43].

^{31}P and ^{1}H MR spectra showed an increase in PC levels to 202±35% of control with 17-AAG treatment, from 17.0±3.0 fmol/cell in control cells to 34.3±4.0 fmol/cell in treated cells (n=3, p=0.005). There was also a significant increase in GPC levels to 214±30% of control with 17-AAG treatment, from 3.7±0.3 fmol/cell in control cells to 8.0±1.7 fmol/cell in treated cells (n=3, p=0.04). Finally, intracellular choline levels were elevated to 194±81% of control with treatment, from 1.1±0.5 fmol/cell in control cells to 2.1±0.8 fmol/cell in 17-AAG treated cells, although this change did not reach statistical significance (n=3, p=0.15). Thus, the effect of 17-AAG on choline-containing metabolite levels was comparable (within experimental error) in cells cultured at physiological choline concentrations and cells cultured with 56 μM choline.

DISCUSSION

In our study, we examined the effects of Hsp90 inhibition on choline metabolism by treating MCF-7 breast cancer cells with the clinically relevant Hsp90 inhibitor, 17-AAG. We found that 17-AAG treatment of MCF-7 cells results in an increase in intracellular choline, PC and GPC concentrations at both normal cell culture and physiological extracellular choline concentrations. We also found that the most significant effect of 17-AAG on the enzymes associated with choline metabolism was an upregulation in expression of choline transporter SLC44A1 and PLA2.

In mammalian cells, choline is actively transported into the cell by various organic cation transporters [34, 35]. The four main proteins responsible for choline transport in human cells are: SLC5A7 (high-affinity choline transporter), SLC44A1 (intermediate affinity choline transporter-like protein), and SLC22A1 and SLC22A2 (polyspecific organic-cation transporters with a very low affinity for choline). SLC44A1

is ubiquitously expressed in human tissues, implying that it is involved in choline metabolism for a broad purpose, such as phospholipid synthesis [44-47]. In MCF-7 cells, SLC44A1 is the most commonly expressed choline transporter (with mRNA expression levels 2 -3 fold higher than SLC22A1/2 and more than thirty-fold higher than SLC5A7 [16]) and is localized on both the plasma and mitochondrial membranes [48]. In our study, 17-AAG did not cause significant changes in SLC5A7, SLC22A1 or SLC22A2, but did significantly increase expression of SLC44A1. Choline transport has been shown to be the rate-limiting step in the two-step formation of PC in breast cancer cell lines, including MCF-7 [49]. Since transport of choline into the cells is slower than phosphorylation of choline, an increase in choline transport would result in an increase in the synthesis of PC. Indeed, in our study no significant changes in choline kinase expression or activity were observed following 17-AAG treatment, ruling out the contribution of ChoK to the increased PC pool. The overexpression of choline transporter SLC44A1 is thus the most likely explanation for an increase in choline transport into the cell, which would result in increased intracellular choline and *de novo* synthesis of PC following 17-AAG treatment.

The link between Hsp90 inhibition and increased SLC44A1 expression remains to be determined. Hsp90 is a chaperone protein with an extremely wide range of client proteins, including those with critical roles in signal transduction, cellular trafficking, chromatin remodeling, cell growth, differentiation and reproduction [50]. With such a global effect on protein and gene expression, the metabolic changes observed could be due to a wide variety of causes. Studies on SLC44A1 are limited, with some indications that Sp1 and/or glucocorticoid receptor may play a role in its transcription [51-54]. However, neither of these transcription factors likely mediates the effect observed here as both were reported to require active Hsp90 for their function, and treatment with the 17-

AAG analogue geldanamycin abrogates their transcriptional activity [53, 55]. Further studies are necessary to link the effect of Hsp90 to the regulation of choline transport.

Aside from the *de novo* synthesis of PC, there are two other potential mechanisms that could contribute to PC accumulation: a decrease in the further metabolism of PC via CCT and an increase in the breakdown of PtdCho. We found no significant change in CCT expression or activity. Although CCT activity can be modulated by relocalization [56] or by changes in substrate concentration, the biological assay findings are consistent with the MRS data, in which there was no modulation in total PtdCho levels. This result is also in line with the fact that CCT is considered the overall rate-limiting step in the synthesis of PtdCho [36]. With regard to breakdown of PtdCho, the expression of PLD increased to 137% following treatment. PLD could generate additional intracellular choline and possibly contribute to PC synthesis. However, the fact that essentially the entire intracellular choline pool was labeled following 48 hours of exposure to labeled choline makes this contribution unlikely. The activity of PLC, which could directly generate PC, dropped following 17-AAG treatment to 66±10% of control. Thus, although modulation of the phospholipases could theoretically have a contribution to the increase in PC, the live cell and extract MRS data showing increases in total PC and *de novo* PC synthesis to the same extent, along with mRNA expression showing increased SLC44A1 expression to a similar degree, favor an increase in choline transport as being the primary mechanism for increased intracellular choline and PC.

Regarding the observed increase in total and *de novo* GPC following 17-AAG treatment, we observed an increase in the activity of the PtdCho-specfic PLA2 and microarray data showed an increase in five of the PLA2 isoenzymes. Thus, the increase in GPC is likely due to increased PtdCho breakdown in treated cells. Activation of PLA2 was also observed in response to other types of therapy [33]. However, we did not

observe a significant change in total PtdCho levels. One possible explanation could be lack of sensitivity: the concentration of PtdCho (25±4 fmol/cell in control cells) is about 5 times greater than the concentration of GPC (4±1 fmol/cell in control cells) and the change in GPC concentration from control to treated cells (an increase of 3.3 fmol/cell) is smaller than the standard deviation in the total PtdCho concentration. It is thus possible that our methods are not sensitive enough to detect such a small change. Alternatively, it is possible that inhibition of PLC (17-AAG caused PLC activity to decrease to 66±10% of control) functions to counteract the elevated breakdown of PtdCho by PLA2, thereby maintaining a constant PtdCho pool.

Our findings are in agreement with the previous studies performed by Chung *et al* on human colon cancer cell lines, which reported an increase in PC concentrations in both cells and tumors when probed either with ^{31}P or ^{1}H MRS [29]. Additionally, our results are in line with an increase in uptake of the PET tracer [^{11}C]-choline reported in MCF-7 cells following Hsp90 inhibition [30]. This study, which measured choline uptake after cells were exposed to [^{11}C]-choline for 30 min, supports our results that inhibition of Hsp90 causes an increase in the transport of choline. An increase in [^{11}C]-choline uptake was also reported in human glioblastoma and human colon cancer cell lines, indicating that the mechanistic findings described here could potentially explain the metabolic effect of 17-AAG in other cancer cell types.

In contrast, Le *et al* reported a decrease in t-Cho levels of prostate cancer xenografts during the first 48 hours of treatment with 17-AAG, as measured by ^{1}H MRSI [57]. Since this was the first investigation of choline-containing metabolite levels following Hsp90 inhibition in a prostate cancer model, it is possible this cancer type responds differently to Hsp90 inhibition. It is also possible that a longer treatment time is necessary to cause an increase in the concentration of PC. Indeed, the drop in PC reported

by Le *et al* was observed within 4 hours of treatment. Similarly, Liu *et al* also reported that treatment with the Hsp90 inhibitor geldanamycin resulted in a drop in PC and a reduction in (methyl-^{14}C) choline uptake within one hour of treatment [58]. These rapid changes in choline uptake are unlikely to involve a change in protein expression, as was the case in our longer study.

CONCLUSIONS

We have shown in our study, for the first time in a breast cancer model, that inhibition of Hsp90 results in a significant, MRS-detectable increase in intracellular choline, PC and GPC. 17-AAG is currently being assessed in multiple clinical trials involving breast cancer patients, including patients that develop resistance to other therapies [2, 5, 59-61]. As Hsp90 inhibitors enter routine clinical use, the value of MRS as a noninvasive and localized imaging method to probe the effects of 17-AAG (and possibly other HSP90 inhibitors) should thus be assessed further. ^{1}H MRSI is an increasingly recognized imaging method, which provides metabolic information that can help distinguish between benign and malignant lesions and inform on tumor response to treatment [62, 63]. The t-Cho peak, which is detectable by ^{1}H MRSI, is comprised of choline, PC and GPC. The substantial increase in all three metabolites observed in this study would thus provide an easily detectable noninvasive biomarker of molecular drug response, which could enhance treatment monitoring and contribute to improved care for breast cancer patients.

ABBREVIATIONS

17-AAG: 17-allyamino-17-demethoxygeldanamycin; Hsp90: Heat Shock Protein 90; MRS: magnetic resonance spectroscopy; MRSI: magnetic resonance spectroscopic imaging; PC: phosphocholine; GPC: glycerophosphocholine; t-Cho: total choline-containg metabolites; ChoK: choline kinase; CCT: CTP:phosphocholine cytidylyltransferase; CDP-choline: cytidine diphosphate-choline; CPT: diacylglycerol cholinephosphotransferase; PtdCho: phosphatidylcholine; PLA: phosphoplipase A; PLC: phospholipase C; PLD: phospholipase D; LPL: lyso-phospholipase; GDPD: glycerophosphocholine phosphodiesterase; BSA: bovine serum albumim; fmol: femtomoles.

COMPETING INTERESTS

The authors declare that they have no competing interests.

AUTHORS' CONTRIBUTIONS

AB acquired, analyzed and interpreted experimental data, contributed to experimental conception and design, and drafted the manuscript. CW acquired and analyzed microarray data, created CTP:PC Cytidylyltransferase Activity Assay and contributed to experimental design. SR conceived of the study, assisted with interpretation of data, and contributed to drafting of the manuscript. All authors have read and approved the final manuscript.

ACKNOWLEDGEMENTS

The authors would like to acknowledge Judy Hwang for assistance with acquisition and analysis of MRS data and Sarah Elmes for assistance with acquisition and analysis of flow cytometry data. This work was supported by NIH grant RO1 CA130819.

REFERENCES

1. Engelman JA: **Targeting PI3K signalling in cancer: opportunities, challenges and limitations.** *Nat Rev Cancer* 2009, **9:**550-562.
2. Solit DB, Rosen N: **Hsp90: a novel target for cancer therapy.** *Curr Top Med Chem* 2006, **6:**1205-1214.
3. Pick E, Kluger Y, Giltnane JM, Moeder C, Camp RL, Rimm DL, Kluger HM: **High HSP90 expression is associated with decreased survival in breast cancer.** *Cancer Res* 2007, **67:**2932-2937.
4. Banerji U: **Heat shock protein 90 as a drug target: some like it hot.** *Clin Cancer Res* 2009, **15:**9-14.
5. Gimenez Ortiz A, Montalar Salcedo J: **Heat shock proteins as targets in oncology.** *Clin Transl Oncol* 2010, **12:**166-173.
6. Song D, Chaerkady R, Tan AC, Garcia-Garcia E, Nalli A, Suarez-Gauthier A, Lopez-Rios F, Zhang XF, Solomon A, Tong J, Read M, Fritz C, Jimeno A, Pandey A, Hidalgo M: **Antitumor activity and molecular effects of the novel heat shock protein 90 inhibitor, IPI-504, in pancreatic cancer.** *Mol Cancer Ther* 2008, **7:**3275-3284.

7. Lang SA, Klein D, Moser C, Gaumann A, Glockzin G, Dahlke MH, Dietmaier W, Bolder U, Schlitt HJ, Geissler EK, Stoeltzing O: **Inhibition of heat shock protein 90 impairs epidermal growth factor-mediated signaling in gastric cancer cells and reduces tumor growth and vascularization in vivo.** *Mol Cancer Ther* 2007, **6:**1123-1132.

8. Banerji U, Walton M, Raynaud F, Grimshaw R, Kelland L, Valenti M, Judson I, Workman P: **Pharmacokinetic-pharmacodynamic relationships for the heat shock protein 90 molecular chaperone inhibitor 17-allylamino, 17-demethoxygeldanamycin in human ovarian cancer xenograft models.** *Clin Cancer Res* 2005, **11:**7023-7032.

9. Beckonert O, Monnerjahn J, Bonk U, Leibfritz D: **Visualizing metabolic changes in breast-cancer tissue using 1H-NMR spectroscopy and self-organizing maps.** *NMR Biomed* 2003, **16:**1-11.

10. Glunde K, Jie C, Bhujwalla ZM: **Molecular causes of the aberrant choline phospholipid metabolism in breast cancer.** *Cancer Res* 2004, **64:**4270-4276.

11. Ramirez de Molina A, Banez-Coronel M, Gutierrez R, Rodriguez-Gonzalez A, Olmeda D, Megias D, Lacal JC: **Choline kinase activation is a critical requirement for the proliferation of primary human mammary epithelial cells and breast tumor progression.** *Cancer Res* 2004, **64:**6732-6739.

12. Glunde K, Jacobs MA, Pathak AP, Artemov D, Bhujwalla ZM: **Molecular and functional imaging of breast cancer.** *NMR Biomed* 2009, **22:**92-103.

13. Ting YL, Sherr D, Degani H: **Variations in energy and phospholipid metabolism in normal and cancer human mammary epithelial cells.** *Anticancer Res* 1996, **16:**1381-1388.

14. Negendank W: **Studies of human tumors by MRS: a review.** *NMR Biomed* 1992, **5:**303-324.

15. Aboagye EO, Bhujwalla ZM: **Malignant transformation alters membrane choline phospholipid metabolism of human mammary epithelial cells.** *Cancer Res* 1999, **59:**80-84.

16. Eliyahu G, Kreizman T, Degani H: **Phosphocholine as a biomarker of breast cancer: molecular and biochemical studies.** *Int J Cancer* 2007, **120:**1721-1730.

17. Bhujwalla ZM: **Molecular and functional imaging of cancer.** *Conf Proc IEEE Eng Med Biol Soc* 2009, **2009:**47-49.

18. Beloueche-Babari M, Chung YL, Al-Saffar NM, Falck-Miniotis M, Leach MO: **Metabolic assessment of the action of targeted cancer therapeutics using magnetic resonance spectroscopy.** *Br J Cancer* 2010, **102:**1-7.

19. Gottschalk S, Anderson N, Hainz C, Eckhardt SG, Serkova NJ: **Imatinib (STI571)-mediated changes in glucose metabolism in human leukemia BCR-ABL-positive cells.** *Clin Cancer Res* 2004, **10:**6661-6668.

20. Jordan BF, Black K, Robey IF, Runquist M, Powis G, Gillies RJ: **Metabolite changes in HT-29 xenograft tumors following HIF-1alpha inhibition with PX-478 as studied by MR spectroscopy in vivo and ex vivo.** *NMR Biomed* 2005, **18:**430-439.

21. Beloueche-Babari M, Jackson LE, Al-Saffar NM, Workman P, Leach MO, Ronen SM: **Magnetic resonance spectroscopy monitoring of mitogen-activated protein kinase signaling inhibition.** *Cancer Res* 2005, **65:**3356-3363.

22. Al-Saffar NM, Troy H, Ramirez de Molina A, Jackson LE, Madhu B, Griffiths JR, Leach MO, Workman P, Lacal JC, Judson IR, Chung YL: **Noninvasive magnetic resonance spectroscopic pharmacodynamic markers of the choline**

kinase inhibitor MN58b in human carcinoma models. *Cancer Res* 2006, **66:**427-434.

23. Beloueche-Babari M, Jackson LE, Al-Saffar NM, Eccles SA, Raynaud FI, Workman P, Leach MO, Ronen SM: **Identification of magnetic resonance detectable metabolic changes associated with inhibition of phosphoinositide 3-kinase signaling in human breast cancer cells.** *Mol Cancer Ther* 2006, **5:**187-196.

24. Kominsky DJ, Klawitter J, Brown JL, Boros LG, Melo JV, Eckhardt SG, Serkova NJ: **Abnormalities in glucose uptake and metabolism in imatinib-resistant human BCR-ABL-positive cells.** *Clin Cancer Res* 2009, **15:**3442-3450.

25. Ward CS, Venkatesh HS, Chaumeil MM, Brandes AH, Vancriekinge M, Dafni H, Sukumar S, Nelson SJ, Vigneron DB, Kurhanewicz J, James CD, Haas-Kogan DA, Ronen SM: **Noninvasive detection of target modulation following phosphatidylinositol 3-kinase inhibition using hyperpolarized 13C magnetic resonance spectroscopy.** *Cancer Res* 2010, **70:**1296-1305.

26. Ross J, Najjar AM, Sankaranarayanapillai M, Tong WP, Kaluarachchi K, Ronen SM: **Fatty acid synthase inhibition results in a magnetic resonance-detectable drop in phosphocholine.** *Mol Cancer Ther* 2008, **7:**2556-2565.

27. Muruganandham M, Alfieri AA, Matei C, Chen Y, Sukenick G, Schemainda I, Hasmann M, Saltz LB, Koutcher JA: **Metabolic signatures associated with a NAD synthesis inhibitor-induced tumor apoptosis identified by 1H-decoupled-31P magnetic resonance spectroscopy.** *Clin Cancer Res* 2005, **11:**3503-3513.

28. Glunde K, Jie C, Bhujwalla ZM: **Mechanisms of indomethacin-induced alterations in the choline phospholipid metabolism of breast cancer cells.** *Neoplasia* 2006, **8:**758-771.

29. Chung YL, Troy H, Banerji U, Jackson LE, Walton MI, Stubbs M, Griffiths JR, Judson IR, Leach MO, Workman P, Ronen SM: **Magnetic resonance spectroscopic pharmacodynamic markers of the heat shock protein 90 inhibitor 17-allylamino,17-demethoxygeldanamycin (17AAG) in human colon cancer models.** *J Natl Cancer Inst* 2003, **95:**1624-1633.

30. Monazzam A, Razifar P, Ide S, Rugaard Jensen M, Josephsson R, Blomqvist C, Langstrom B, Bergstrom M: **Evaluation of the Hsp90 inhibitor NVP-AUY922 in multicellular tumour spheroids with respect to effects on growth and PET tracer uptake.** *Nucl Med Biol* 2009, **36:**335-342.

31. Delikatny E, Roman S, Hancock R, Jeitner T, Lander C, Rideout D, Mountford C: **Tetraphenylphosphonium chloride induced MR-visible lipid accumulation in a malignant human breast cell line.** *Int J Cancer* 1996, **67:**72-79.

32. Milkevitch M, Shim H, Pilatus U, Pickup S, Wehrle J, Samid D, Poptani H, Glickson J, Delikatny E: **Increases in NMR-visible lipid and glycerophosphocholine during phenylbutyrate-induced apoptosis in human prostate cancer cells.** *Biochim Biophys Acta* 2005, **1734:**1-12.

33. Liimatainen T, Erkkila A, Valonen P, Vidgren H, Lakso M, Wong G, Grohn O, Yla-Herttuala S, Hakumaki J: **1H MR spectroscopic imaging of phospholipase-mediated membrane lipid release in apoptotic rat glioma in vivo.** *Magn Reson Med* 2008, **59:**1232-1238.

34. Koepsell H, Endou H: **The SLC22 drug transporter family.** *Pflugers Arch* 2004, **447:**666-676.

35. Koepsell H, Schmitt BM, Gorboulev V: **Organic cation transporters.** *Rev Physiol Biochem Pharmacol* 2003, **150:**36-90.

36. Sundler R, Akesson B: **Regulation of phospholipid biosynthesis in isolated rat hepatocytes. Effect of different substrates.** *J Biol Chem* 1975, **250:**3359-3367.

37. Ronen SM, Rushkin E, Degani H: **Lipid metabolism in T47D human breast cancer cells: 31P and 13C-NMR studies of choline and ethanolamine uptake.** *Biochim Biophys Acta* 1991, **1095:**5-16.

38. Ronen SM, DiStefano F, McCoy CL, Robertson D, Smith TA, Al-Saffar NM, Titley J, Cunningham DC, Griffiths JR, Leach MO, Clarke PA: **Magnetic resonance detects metabolic changes associated with chemotherapy-induced apoptosis.** *Br J Cancer* 1999, **80:**1035-1041.

39. Tyagi RK, Azrad A, Degani H, Salomon Y: **Simultaneous extraction of cellular lipids and water-soluble metabolites: evaluation by NMR spectroscopy.** *Magn Reson Med* 1996, **35:**194-200.

40. Iorio E, Mezzanzanica D, Alberti P, Spadaro F, Ramoni C, D'Ascenzo S, Millimaggi D, Pavan A, Dolo V, Canevari S, Podo F: **Alterations of choline phospholipid metabolism in ovarian tumor progression.** *Cancer Res* 2005, **65:**9369-9376.

41. Vance DE, Pelech SD, Choy PC: **CTP: phosphocholine cytidylyltransferase from rat liver.** *Methods Enzymol* 1981, **71 Pt C:**576-581.

42. Savendahl L, Mar MH, Underwood LE, Zeisel SH: **Prolonged fasting in humans results in diminished plasma choline concentrations but does not cause liver dysfunction.** *Am J Clin Nutr* 1997, **66:**622-625.

43. Zeisel SH, Growdon JH, Wurtman RJ, Magil SG, Logue M: **Normal plasma choline responses to ingested lecithin.** *Neurology* 1980, **30:**1226-1229.

44. Michel V, Yuan Z, Ramsubir S, Bakovic M: **Choline transport for phospholipid synthesis.** *Exp Biol Med (Maywood)* 2006, **231:**490-504.

45. Blusztajn JK, Wurtman RJ: **Choline and cholinergic neurons.** *Science* 1983, **221:**614-620.

46. Wille S, Szekeres A, Majdic O, Prager E, Staffler G, Stockl J, Kunthalert D, Prieschl EE, Baumruker T, Burtscher H, Zlabinger GJ, Knapp W, Stockinger H: **Characterization of CDw92 as a member of the choline transporter-like protein family regulated specifically on dendritic cells.** *J Immunol* 2001, **167:**5795-5804.

47. Machova E, O'Regan S, Newcombe J, Meunier FM, Prentice J, Dove R, Lisa V, Dolezal V: **Detection of choline transporter-like 1 protein CTL1 in neuroblastoma x glioma cells and in the CNS, and its role in choline uptake.** *J Neurochem* 2009, **110:**1297-1309.

48. Michel V, Bakovic M: **The solute carrier 44A1 is a mitochondrial protein and mediates choline transport.** *FASEB J* 2009, **23:**2749-2758.

49. Katz-Brull R, Degani H: **Kinetics of choline transport and phosphorylation in human breast cancer cells; NMR application of the zero trans method.** *Anticancer Res* 1996, **16:**1375-1380.

50. Zuehlke A, Johnson JL: **Hsp90 and co-chaperones twist the functions of diverse client proteins.** *Biopolymers* 2010, **93:**211-217.

51. Fullerton MD, Wagner L, Yuan Z, Bakovic M: **Impaired trafficking of choline transporter-like protein-1 at plasma membrane and inhibition of choline transport in THP-1 monocyte-derived macrophages.** *Am J Physiol Cell Physiol* 2006, **290:**C1230-1238.

52. Yuan Z, Tie A, Tarnopolsky M, Bakovic M: **Genomic organization, promoter activity, and expression of the human choline transporter-like protein 1.** *Physiol Genomics* 2006, **26:**76-90.

53. Wang SA, Chuang JY, Yeh SH, Wang YT, Liu YW, Chang WC, Hung JJ: **Heat shock protein 90 is important for Sp1 stability during mitosis.** *J Mol Biol* 2009, **387:**1106-1119.

54. Nakamura T, Fujiwara R, Ishiguro N, Oyabu M, Nakanishi T, Shirasaka Y, Maeda T, Tamai I: **Involvement of choline transporter-like proteins, CTL1 and CTL2, in glucocorticoid-induced acceleration of phosphatidylcholine synthesis via increased choline uptake.** *Biol Pharm Bull* 2010, **33:**691-696.

55. Kang KI, Meng X, Devin-Leclerc J, Bouhouche I, Chadli A, Cadepond F, Baulieu EE, Catelli MG: **The molecular chaperone Hsp90 can negatively regulate the activity of a glucocorticosteroid-dependent promoter.** *Proc Natl Acad Sci U S A* 1999, **96:**1439-1444.

56. Jackowski S, Fagone P: **CTP: Phosphocholine cytidylyltransferase: paving the way from gene to membrane.** *J Biol Chem* 2005, **280:**853-856.

57. Le HC, Lupu M, Kotedia K, Rosen N, Solit D, Koutcher JA: **Proton MRS detects metabolic changes in hormone sensitive and resistant human prostate cancer models CWR22 and CWR22r.** *Magn Reson Med* 2009, **62:**1112-1119.

58. Liu D, Hutchinson OC, Osman S, Price P, Workman P, Aboagye EO: **Use of radiolabelled choline as a pharmacodynamic marker for the signal transduction inhibitor geldanamycin.** *Br J Cancer* 2002, **87:**783-789.

59. Widakowich C, Dinh P, de Azambuja E, Awada A, Piccart-Gebhart M: **HER-2 positive breast cancer: what else beyond trastuzumab-based therapy?** *Anticancer Agents Med Chem* 2008, **8:**488-496.

60. Dean-Colomb W, Esteva FJ: **Emerging agents in the treatment of anthracycline- and taxane-refractory metastatic breast cancer.** *Semin Oncol* 2008, **35:**S31-38; quiz S40.

61. Powers MV, Workman P: **Targeting of multiple signalling pathways by heat shock protein 90 molecular chaperone inhibitors.** *Endocr Relat Cancer* 2006, **13 Suppl 1:**S125-135.

62. Sinha S, Sinha U: **Recent advances in breast MRI and MRS.** *NMR Biomed* 2009, **22:**3-16.

63. Bolan PJ, Nelson MT, Yee D, Garwood M: **Imaging in breast cancer: Magnetic resonance spectroscopy.** *Breast Cancer Res* 2005, **7:**149-152.

FIGURE CAPTIONS

Figure 1: Schematic of choline phospholipid metabolism. Schematic drawing of choline phospholipid metabolism and its regulatory enzymes illustrating the metabolic reactions associated with modulation of choline-containing metabolites.

Figure 2: Effect of 17-AAG on cell proliferation and Hsp90 client protein levels. (a) Western blot analysis showing depletion of HSP90 client proteins total-Akt and c-Raf following 17-AAG treatment of MCF-7 cells for 48 hours. Actin was used as a loading control. **(b)** Results of WST-1 Assay showing 17-AAG effects on MCF-7 cell proliferation over a 48-hour treatment period.

Figure 3: MRS-detection of increased total and *de novo* PC in live, perfused cells following 17-AAG treatment. (a) ^{31}P spectra of live, perfused MCF-7 cells illustrating an increase in PC after 48 hours of 17-AAG treatment. **(b)** ^{13}C spectral array depicting the buildup of [1,2-^{13}C]-PC in perfused MCF-7 cells over a 14-hour period. **(c)** Graph of buildup of *de novo* [1,2-^{13}C]-PC in control (blue) and 17-AAG-treated (red) MCF-7 cells over 14 hours of exposure to [1,2-^{13}C]-choline. The data represent an average of 3 repeats.

Figure 4: Representative ^{31}P, ^{13}C, and ^{1}H spectra of cell extracts. Representative spectra of control (bottom) and 17-AAG treated (top) MCF-7 cells illustrating increased PC, intracellular choline and GPC levels and unchanged PtdCho levels. **(a)** ^{13}P spectra of the aqueous cell extract fraction depicting an increase in total PC and GPC levels after treatment. **(b)** ^{13}C spectra of the aqueous cell extract fraction depicting an increase in *de novo* synthesized PC, GPC, and intracellular choline. **(c)** ^{31}P spectra of the lipid cell extract fraction depicting constant PtdCho with 17-AAG treatment. **(d)** ^{1}H spectra of the aqueous cell extract fraction depicting an increase in the intracellular choline, PC and GPC concentrations.

TABLE 1: Summary of Microarray Data for Enzymes associated with Choline Metabolism

Enzyme Type	Gene Symbol	Gene Title	% Control	FDR
CHOLINE TRANSPORT				
	SLC5A7	solute carrier family 5 (choline transporter), member 7	101	0.91
	SLC44A1	**solute carrier family 44, member 1**	**154***	**$2.10*10^{-6}$**
	SLC22A1	solute carrier family 22 (organic cation transporter), member 1	99	.97
	SLC22A2	solute carrier family 22 (organic cation transporter), member 2	97	.81
CHOLINE KINASE	CHKA	choline kinase alpha	109	0.2
	CHKB	choline kinase beta	102	0.86
CTP:PC CYTIDYLYLTRANSFERASE	PCYT1A	phosphate cytidylyltransferase 1, choline, alpha	101	0.92
	PCYT1B	phosphate cytidylyltransferase 1, choline, beta	109	0.35
DIACYLGLYCEROL CHOLINE-PHOSPHOTRANSFERASE	**CHPT1**	**choline phosphotransferase 1**	**146***	**$2.4*10^{-4}$**
PHOSPHOLIPASE A	**PLA1A**	**phospholipase A1 member A**	**121***	**0.05**
	PLA2G1B	phospholipase A2, group IB (pancreas)	105	0.67
	PLA2G2A	phospholipase A2, group IIA (platelets, synovial fluid)	101	0.96
	PLA2G2C	phospholipase A2, group IIC	104	0.83
	PLA2G2D	phospholipase A2, group IID	98	0.83
	PLA2G2E	phospholipase A2, group IIE	98	0.91
	PLA2G3	phospholipase A2, group III	99	0.18
	PLA2G4C	**phospholipase A2, group IVC (cytosolic, calcium-independent)**	**75***	**0.0043**
	PLA2G4E	phospholipase A2, group IVE	101	0.95
	PLA2G4F	**phospholipase A2, group IVF**	**82***	**0.018**
	PLA2G5	phospholipase A2, group V	97	0.87
	PLA2G6	phospholipase A2, group VI (cytosolic, calcium-independent)	129	0.0067
	PLA2G7	phospholipase A2, group VII	112	0.3
	PLA2G10	**phospholipase A2, group X**	**712***	**$1.60*10^{-8}$**
	PLA2G12A	**phospholipase A2, group XIIA**	**87***	**0.03**
	PLA2G12B	phospholipase A2, group XIIB	106	0.51
	PLA2G15	phospholipase A2, group XV	139	0.00043
	PLA2G16	phospholipase A2, group XVI	131	0.0021
PHOSPHOLIPASE D	**PLD1**	**phospholipase D1, phosphatidylcholine-specific**	**137***	**0.0038**
	PLD2	phospholipase D2	106	0.68
	PLD3	**phospholipase D family, member 3**	**179***	**$7.80*10^{-7}$**
	PLD4	phospholipase D family, member 4	106	0.68
	PLD5	phospholipase D family, member 5	116	0.1
	PLD6	**phospholipase D family, member 6**	**82***	**0.0036**
LYSO-PHOSPHOLIPASE	LYPLA1	lysophospholipase I	90	0.13
	LYPLAL1	lysophospholipase-like 1	88	0.18
	LYPLA2	lysophospholipase II	90	0.14
GLYCERO PHOSPHOCHOLINE PHOSPHODIESTERASE	GDPD1	glycerophosphodiester phosphodiesterase domain containing 1	106	0.64
	GDPD2	**glycerophosphodiester phosphodiesterase domain containing 2**	**228***	**$1.2*10^{-6}$**

GDPD3	**glycerophosphodiester phosphodiesterase domain containing 3**	**142***	**$2.6*10^{-7}$**
GDPD5	glycerophosphodiester phosphodiesterase domain containing 5	116	0.18
GDE1	glycerophosphodiester phosphodiesterase 1	112	0.062

Enzymes that had a statistically significant (False Discovery Rate (FDR) less than or equal to 0.05) modulation in expression with 17-AAG treatment are indicated with a * and highlighted in bold.

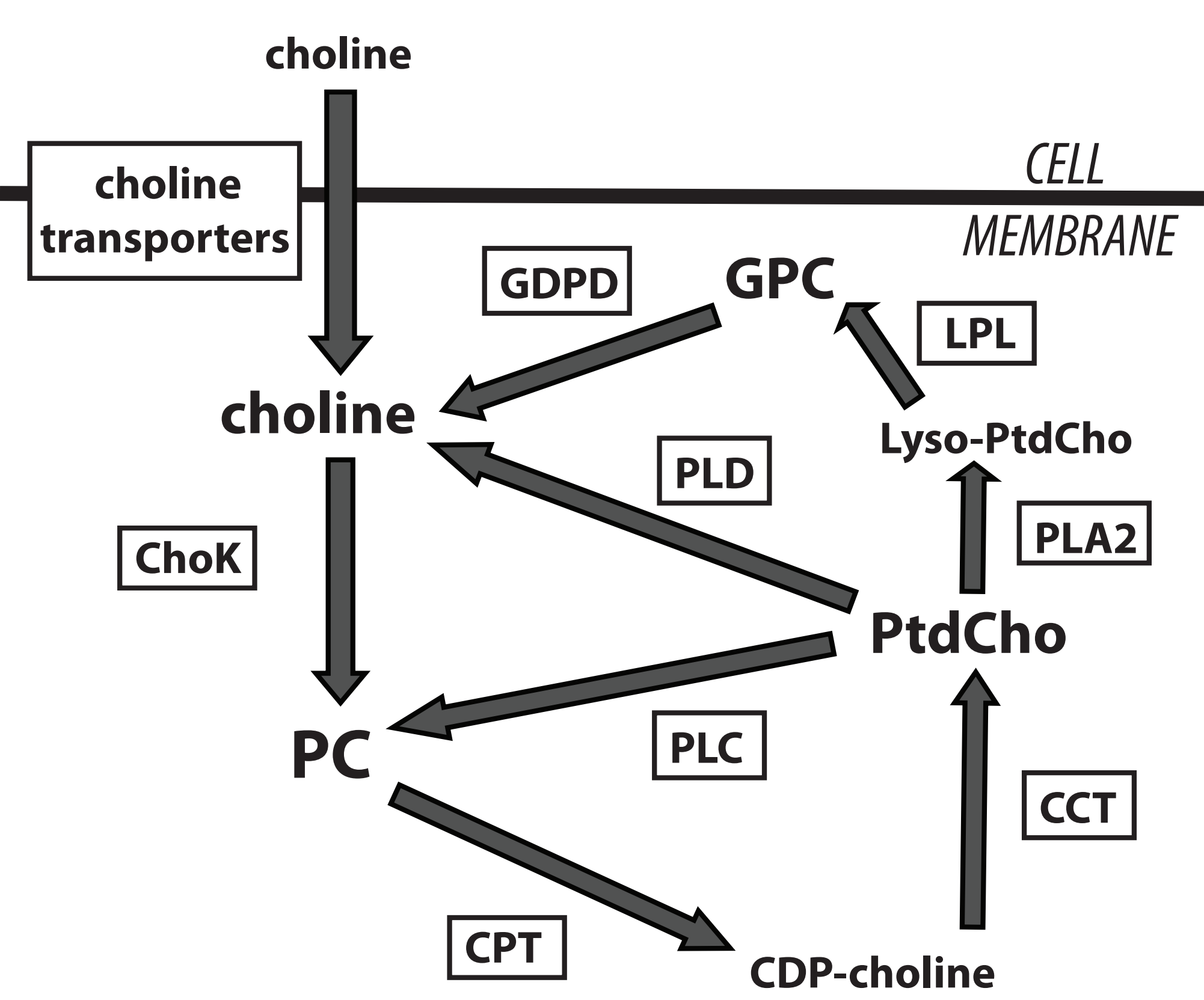
choline
choline transporters
CELL MEMBRANE
GDPD
GPC
LPL
choline
Lyso-PtdCho
PLD
PLA2
ChoK
PtdCho
PC
PLC
CCT
CPT
CDP-choline

Figure 1

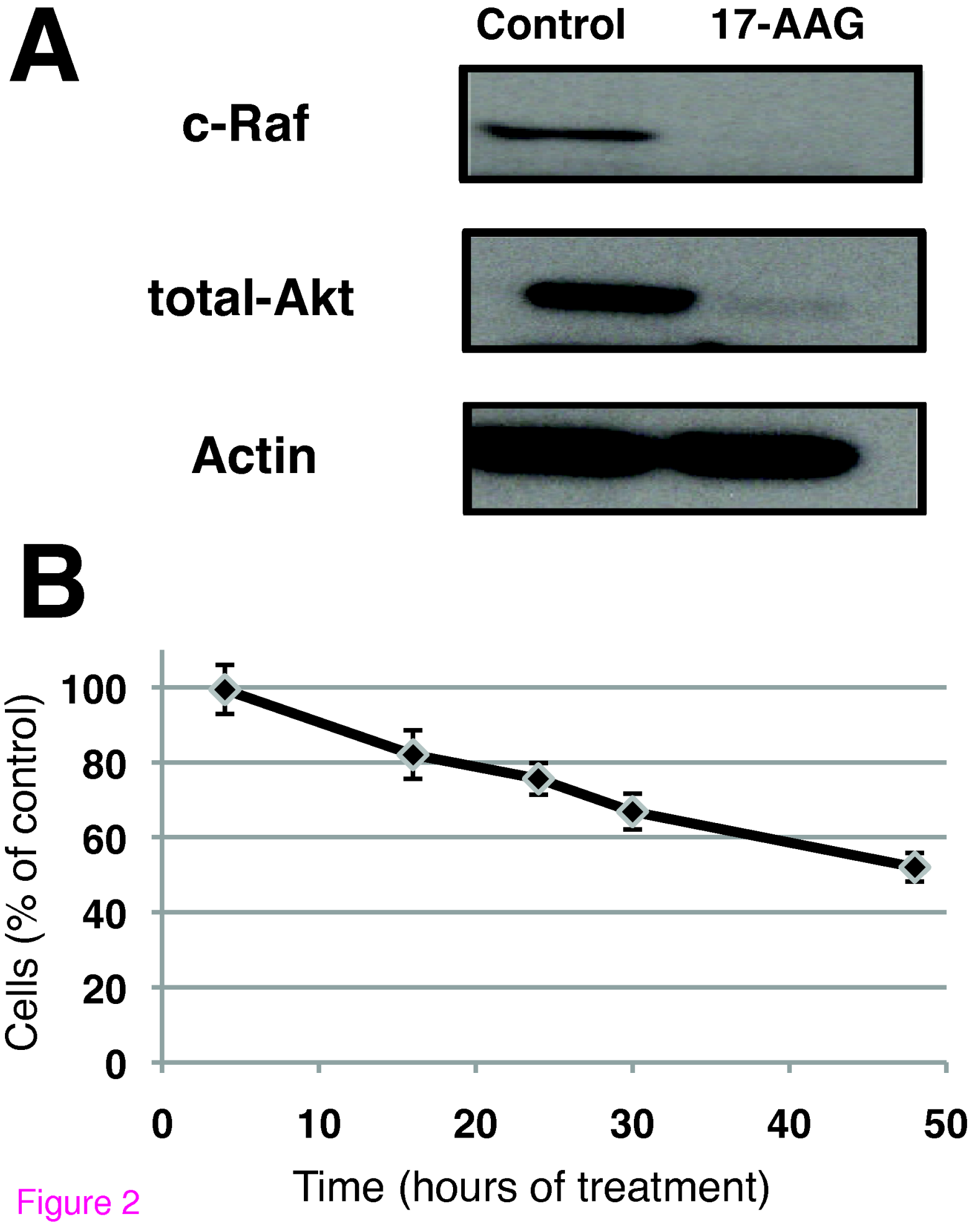
A
Control
17-AAG
c-Raf
total-Akt
Actin
B
Cells (% of control)
100
80
60
40
20
0
0
10
20
30
40
50
Time (hours of treatment)

Figure 2

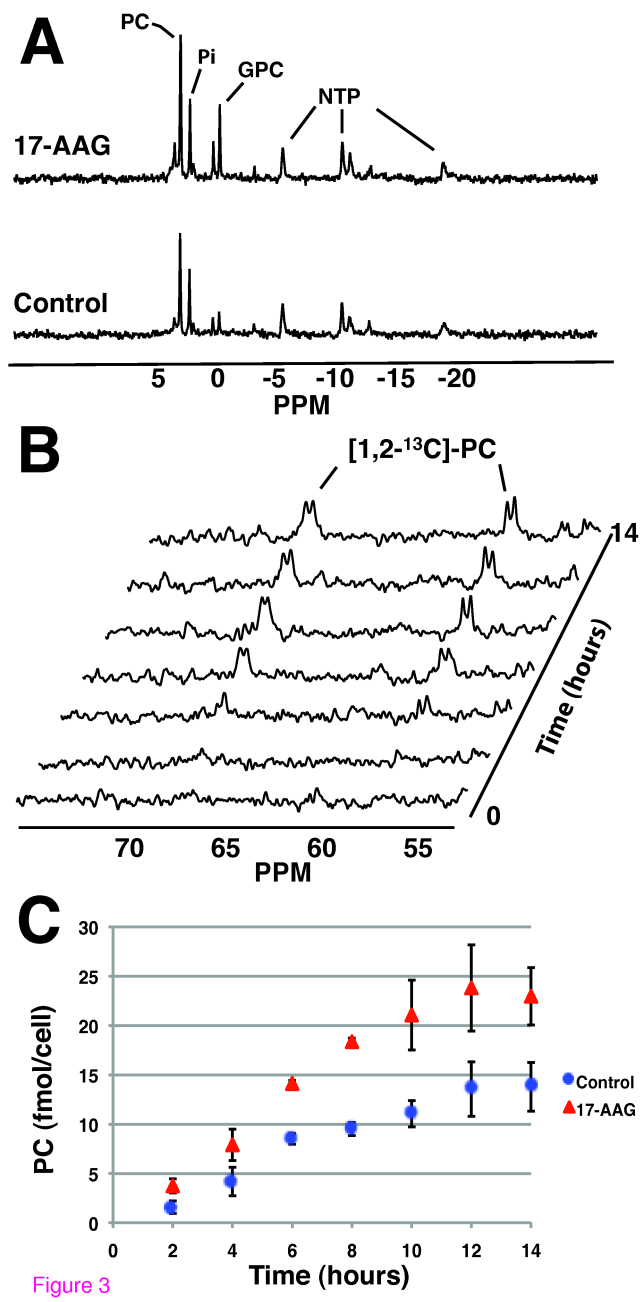
A
PC
Pi
GPC
NTP
17-AAG
Control
5
0
-5
-10
-15
-20
PPM
B
[1,2-13C]-PC
14
Time (hours)
0
70
65
60
55
PPM
C
30
25
20
15
10
5
0
PC (fmol/cell)
0
2
4
6
8
10
12
14
Time (hours)
Control
17-AAG

Figure 3

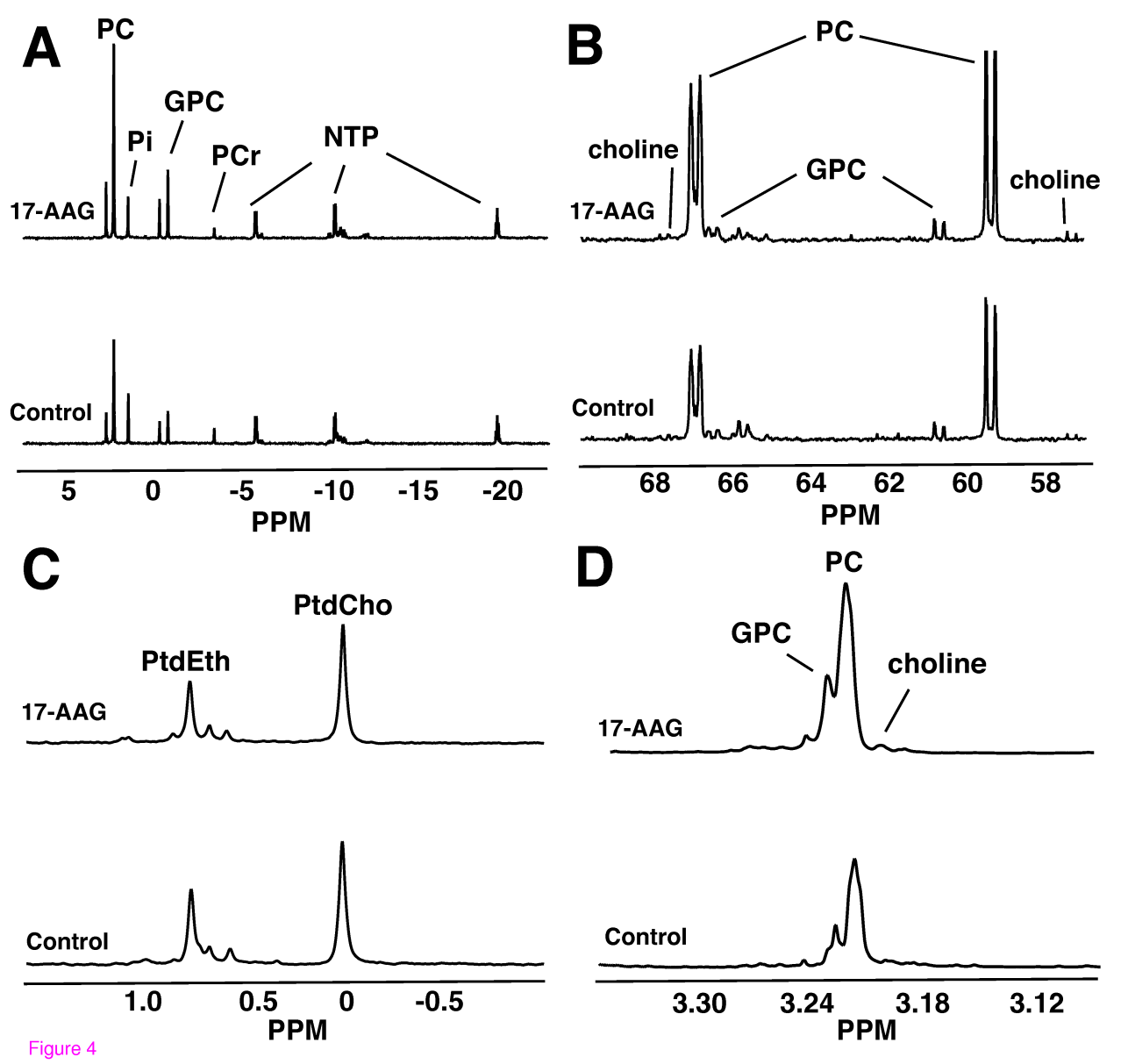
A
PC
Pi
GPC
PCr
NTP
17-AAG
Control
5
0
-5
-10
-15
-20
PPM
B
PC
choline
GPC
choline
17-AAG
Control
68
66
64
62
60
58
PPM
C
PtdCho
PtdEth
17-AAG
Control
1.0
0.5
0
-0.5
PPM
D
PC
GPC
choline
17-AAG
Control
3.30
3.24
3.18
3.12
PPM

Figure 4